Combustion Intermediates in Fuel-Rich 1,4-Dioxane Flame Studied by Tunable Synchrotron Vacuum Ultraviolet Photoionization

Zhenkun Lin,[†] Donglin Han,[†] Shufen Li,*[,†] Yuyang Li,[‡] and Tao Yuan[‡]

Department of Chemical Physics, University of Science and Technology of China, Hefei, Anhui 230026, People's Republic of China, and National Synchrotron Radiation Laboratory, University of Science and Technology of China, Hefei, Anhui 230029, People's Republic of China

Received: November 10, 2008; Revised Manuscript Received: December 31, 2008

Combustion intermediates of a cyclic oxygenated hydrocarbon, 1,4-dioxane, were studied with the tunable synchrotron vacuum ultraviolet photoionization and molecular-beam mass spectrometry (MBMS) technique. A fuel-rich premixed laminar 1,4-dioxane/O_2/Ar flame at low pressure with an equivalence ratio of 1.80 was investigated in the present work. A total of 20 intermediates were observed, and their mole fraction profiles are calculated. Aromatic intermediates were not observed, and this was a prominent difference between the fuel-rich flames of 1,4-dioxane and previously studied noncyclic oxygenated hydrocarbons. The fuel-rich 1,4-dioxane flame could be divided into four zones, and formation routes of the intermediates were proposed. The discussion on the pollutant emissions showed that some light toxic molecules were produced from 1,4-dioxane combustion; however, toxic aromatics and soot emissions were possibly avoided.

Introduction

As a kind of renewable energy source, biomass has been considered as a promising substitute for fossil fuels. Considerable work on the oxidation and combustion of oxygenated hydrocarbons, which are the major components of biomass fuels, has been performed in the past decade.[1−12]

Fisher et al. developed detailed chemical kinetics models for the combustion of two oxygenated hydrocarbons, methyl butanoate and methyl formate.[3] McEnally et al. experimentally studied fuel decomposition and hydrocarbon growth processes of methyl *tert*-butyl ether and related alkyl ethers in soot-producing nonpremixed flames, and they found that unimolecular dissociation was the dominant decomposition process.[5] Ergut et al. conducted an investigation on the evolution of polycyclic aromatic hydrocarbons (PAHs) and other pollutants emitted from one-dimensional ethyl alcohol flames, and they found that ethyl alcohol combustion generated small yields of PAHs, compared with ethylbenzene combustion.[6] Dooley et al. studied the autoignition of methyl butanoate at 1 and 4 atm in a shock tube over the temperature range of 1250−1760 K, and the autoignition of methyl butanoate was observed to follow Arrhenius-like temperature dependence over all conditions studied.[11]

Recently, the combination of tunable synchrotron vacuum ultraviolet (VUV) photoionization with molecular-beam mass spectrometry (MBMS) has been developed to investigate combustion chemistry.[13−16] Since incomplete combustion produces large numbers of toxic chemicals,[17,18] a series of fuel-rich flames, including that of oxygenated hydrocarbons,[19−22] were studied by this combined technique. For example, Cool et al. identified combustion intermediates and dominant reactions in fuel-rich dimethyl ether (DME) flames, and their studies extended previous measurements of premixed DME/O_2/Ar to include a dozen additional flame species;[19] Li et al. studied fuel-rich flames of acetone, *n*-propyl alcohol, and isopropyl alcohol together with their fuel-lean flames, and it was concluded that different structural features of fuel led to variations in intermediate pools, isomeric compositions, and formation channels of flame species.[21]

Though oxidation and combustion of oxygenated hydrocarbon have been widely studied by varied methods as mentioned above, few investigations have been performed on cyclic oxygenated hydrocarbons. Battin et al. reported an experimental investigation of oxidation of equimolecular mixtures 1,4-dioxane/O_2 in the early 1990s.[23] The investigation showed that 1,4-dioxane reacted with oxygen more readily than most hydrocarbons, and a radical chain mechanism was suggested and discussed. Besides, few investigations have been reported on oxidation and combustion of cyclic oxygenated hydrocarbons as far we know. In comparison with noncyclic oxygenated hydrocarbons, we know much less about the combustion chemistry of cyclic oxygenated hydrocarbons. Therefore, more and in-depth research on the combustion of cyclic oxygenated hydrocarbons is especially important and urgent.

In the present work, a fuel-rich premixed laminar 1,4-dioxane/O_2/Ar flame with an equivalence ratio of 1.80 is studied with the tunable synchrotron VUV photoionization and MBMS technique. Combustion intermediates in fuel-rich 1,4-dioxane flame are identified, and their mole fraction profiles are also evaluated to help understand the combustion chemistry of 1,4-dioxane. Formation routes of combustion intermediates and the characteristics of fuel-rich 1,4-dioxane flame will be discussed. Meanwhile, the pollutant emissions from 1,4-dioxane combustion will be specially considered.

Experimental Methods

The experiments were carried out at the flame endstation of the National Synchrotron Radiation Laboratory (NSRL) in Hefei, China. Detailed descriptions about the instrument have been reported previously.[15,20,24] Briefly, it consists of a low-pressure

* Corresponding author. E-mail: lsf@ustc.edu.cn. Fax: +86-551-3631760. Tel.: +86-551-3601137.
[†] Department of Chemical Physics.
[‡] National Synchrotron Radiation Laboratory.

10.1021/jp8098895 CCC: $40.75
Published on Web 02/09/2009

flame chamber, a differentially pumped molecular-beam sampling system, and a reflectron time-of-flight mass spectrometer (RTOFMS).

Low-pressure laminar premixed 1,4-dioxane/O_2/Ar flame is stabilized on a 6.0 cm diameter McKenna flat burner (Holthuis and Associates, Sebastopol CA). Flame species are sampled through a quartz conelike nozzle with an orifice diameter of ~0.5 mm. The molecular beam of the sampled gases passes through a nickel skimmer into a differentially pumped ionization region. The molecular beam is crossed by the tunable synchrotron VUV light in the photoionization chamber, and then the photoions are collected and analyzed by the RTOFMS with mass resolution ($m/\Delta m$) of ~1400. Movement of the burner toward or away from the quartz nozzle allows the mass spectrum to be taken at different positions in the flame. The synchrotron radiation from a bending magnet beamline of the 800 MeV electron storage ring is dispersed by a 1 m Seya-Namioka monochromator equipped with a 1200 grooves·mm^{-1} grating (Horiba Jobin Yvon, Longjumeau, France). The energy resolution power ($E/\Delta E$) is about 500 with ~150 μm entrance and exit slits. A MgF_2 window is mounted between the exit slit and the photoionization chamber to eliminate the higher-order harmonic radiation when the wavelength is longer than 110 nm.

The flux-normalized ion signals, measured as a function of the photon energy, yielded photoionization efficiency (PIE) spectra. In the present experiment, the quartz nozzle was located at the distance of 6.5 mm from the burner surface to take PIE spectra. The photon wavelengths changed from 118 nm (10.50 eV) to 165 nm (7.55 eV), with a step width of 0.35 nm. The experimental error for determining ionization energy (IE) should be within ±0.05 eV for species with strong signals and ±0.10 eV for species with weak signals as the cooling effect of the molecular beam is considered. In order to obtain accurate mole fractions of most species, the influence of fragment ions from other species should be avoided to maintain near-threshold ionization. Therefore, we scanned the burner position at selected photon energies of 16.53, 14.59, 13.19, 11.81, 11.27, 10.48, 10.00, 9.50, and 9.00 eV. The mole fractions of combustion intermediates were evaluated according to the method described by Cool et al.[25] Photoionization cross sections of most combustion intermediates are available for mole fraction calculations.[14,26−28] For those intermediates with unknown photoionization cross sections, a method reported by Koizumi was used to estimate the cross section values.[29]

The 1,4-dioxane used in the present experiment was supplied by Sinopharm Chemical Reagent Co., Ltd., Shanghai, China. The purity of 1,4-dioxane was 99.5%. An ISCO 1000D syringe pump (Teledyne Isco, Inc., Lincoln NE) was employed to inject 1,4-dioxane to the vaporizer with a liquid flow rate of 1.074 mL·min^{-1} at room temperature. The gas flow rates for O_2 and Ar were 0.784 and 1.066 standard liters per minute (SLM), respectively. Hence, the equivalence ratio (ϕ) and C/O ratio were calculated to be 1.80 and 0.53, respectively. The pressure in the flame chamber is 4.00 kPa (30 Torr).

Results and Discussion

1. Identification of Combustion Intermediates. The photoionization mass spectrum of the investigated fuel-rich 1,4-dioxane flame is shown in Figure 1. It is sampled at a position of 6.5 mm from the burner surface with a photon energy of 10.48 eV. A series of mass peaks can be observed in Figure 1, with the m/z range from 15 to 89. Each mass peak is possibly corresponding to one or more combustion intermediates in fuel-rich 1,4-dioxane flame, and the number of possible isomers

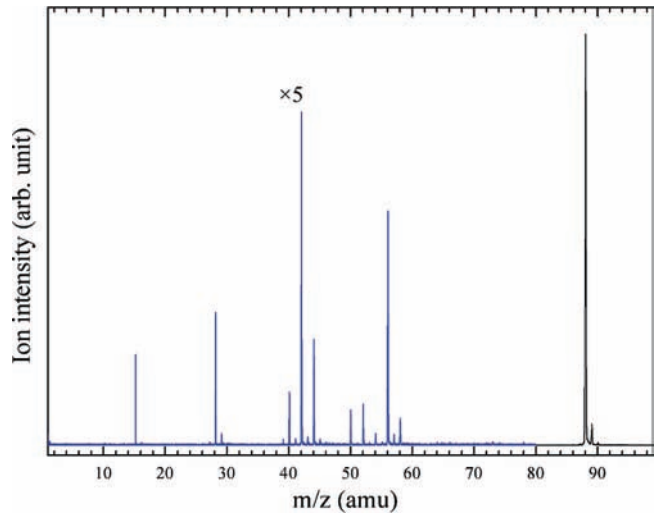

Figure 1. Photoionization mass spectrum of fuel-rich 1,4-dioxane flame with a photon energy of 10.48 eV, taken at 6.5 mm from the burner surface.

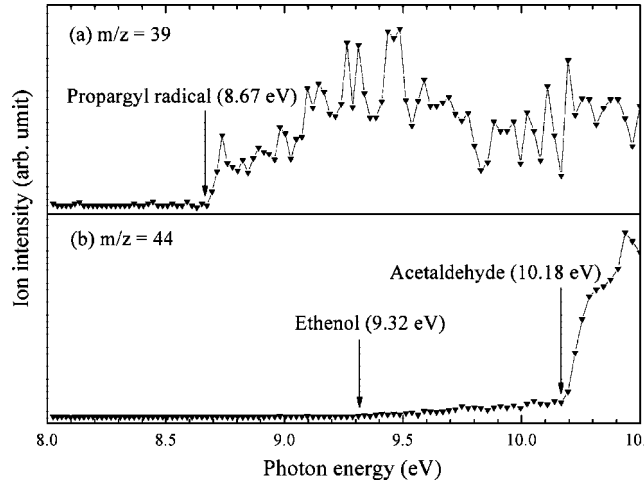

Figure 2. PIE spectra of m/z 39 (a) and m/z 44 (b) in fuel-rich 1,4-dioxane flame.

increases rapidly as the value of m/z increases. However, some of these mass peaks may be corresponding to the fragment ions from fuel and large intermediates or contain the contributions of fragment ions. The interference of fragment ions can be avoided by selecting the photon energy appropriately if the IE of one combustion intermediate is not excessively near to the appearance potential (AP) of the corresponding fragment ion. Isotopes may also interfere with the identification of combustion intermediates. For example, the mass peak of m/z 89 corresponds to the fuel 1,4-dioxane ($C_4H_8O_2$) with one ^{13}C atom. Interference of isotopes can be easily eliminated since the natural abundances of most isotopes in nature are already known.

PIE spectra can provide precise information of ionization thresholds for the isomer-specific identification of combustion intermediates. Figure 2 presents two illustrations of combustion intermediates identification. A clear threshold can be observed at 8.67 eV for the m/z 39 as shown in Figure 2a, which is in good accordance with the literature IE of propargyl radical (IE = 8.67 eV).[30] Two thresholds can be observed at 9.32 and 10.18 eV for the m/z 44 as shown in Figure 2b, which are in good agreement to the literature IEs of ethenol (IE = 9.33 eV)[30] and acetaldehyde (IE = 10.22 eV),[30] respectively. The identified intermediates are listed in Table 1, along with the measured and literature values of IEs, peak positions, and maximum mole

TABLE 1: Combustion Intermediates Identified in the Fuel-Rich 1,4-Dioxane Flame, Along with Their Measured IEs, Peak Positions, and Peak Mole Fractions (X_{Peak})

				IE (eV)		mole fraction	
label	mass	formula	species	this work[a]	literature[b]	peak position (mm)	X_{Peak}
(1)	15	CH_3	methyl radical	9.81	9.84	7.0	1.95×10^{-3}
(2)	26	C_2H_2	acetylene	11.27−11.81[c]	11.40	6.5	2.05×10^{-2}
(3)	28	C_2H_4	ethylene	10.47	10.51	5.0	4.09×10^{-2}
(4)	29	HCO	formyl radical	8.12	8.12	5.5	8.00×10^{-4}[d]
(5)	29	C_2H_5	ethyl radical	8.33	8.26		
(6)	30	H_2CO	formaldehyde	10.48−11.27[c]	10.88	5.0	2.82×10^{-2}
(7)	39	C_3H_3	propargyl radical	8.67	8.67	7.5	3.64×10^{-4}
(8)	40	C_3H_4	allene	9.74	9.69	7.5	1.39×10^{-4}
(9)	40	C_3H_4	propyne	10.34	10.36	8.0	1.55×10^{-4}
(10)	41	C_3H_5	allyl radical	8.14	8.14	6.5	2.73×10^{-4}
(11)	42	C_2H_2O	ketene	9.59	9.62	6.5	3.98×10^{-3}
(12)	44	C_2H_4O	ethenol[e]	9.32	9.33		
(13)	44	C_2H_4O	acetaldehyde[e]	10.18	10.22		
(14)	45	C_2H_5O	ethoxy radical[e]	9.03	9.11		
(15)	50	C_4H_2	1,3-butadiyne	10.14	10.17	9.0	2.29×10^{-4}
(16)	52	C_4H_4	vinylacetylene	9.56	9.58	7.5	1.10×10^{-4}
(17)	54	C_4H_6	1,3-butadiene	9.07	9.07	6.0	1.98×10^{-4}
(18)	56	C_3H_4O	methylketene	8.95	8.95	5.5	7.99×10^{-4}
(19)	56	C_3H_4O	acrolein	10.08	10.11	5.5	2.57×10^{-3}
(20)	58	C_3H_6O	methoxyethylene[e]	8.92	8.95		

[a] Experimental error is ±0.05 eV for species with strong signals and ±0.10 eV for species with weak signals. [b] Refers to ref 30. [c] The IE is determined according to the photoionization mass spectra from scanning burner position. [d] Total maximum mole fraction of the corresponding *m/z* ratio. [e] The peak position and maximum mole fraction are not obtained in the present work.

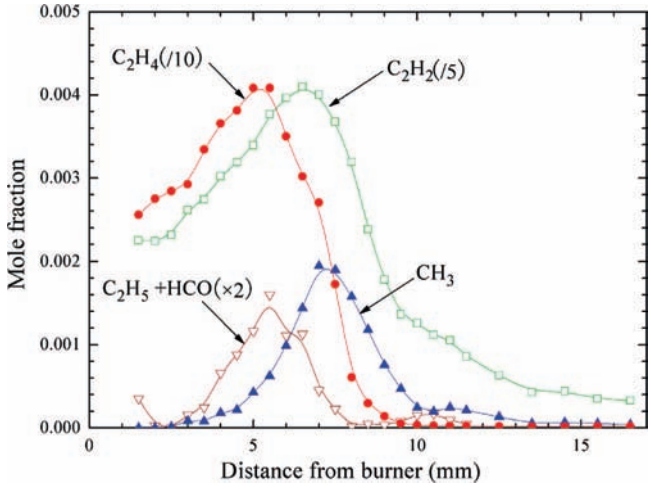

Figure 3. Mole fraction profiles of C_1- and C_2-hydrocarbon intermediates in fuel-rich 1,4-dioxane flame.

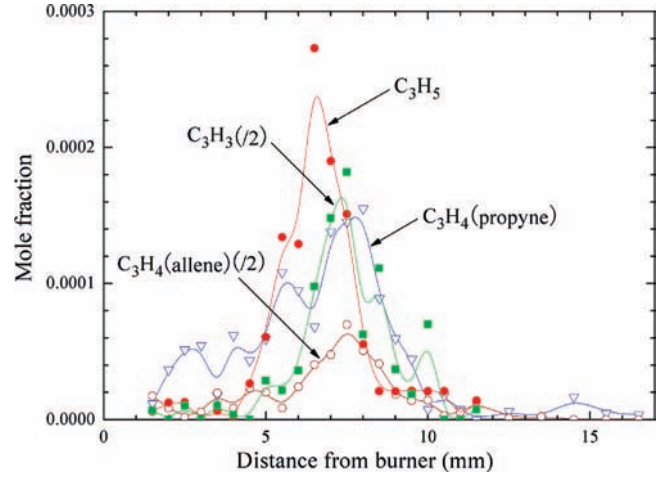

Figure 4. Mole fraction profiles of C_3-hydrocarbon intermediates in fuel-rich 1,4-dioxane flame.

fractions. IEs of acetylene and formaldehyde are higher than the selected photon energies for determining IE in the present work, and they are identified according to the photoionization mass spectrum from scanning burner position. IEs of a few identified intermediates are so near to the APs of the corresponding fragment ions that their peak positions and maximum mole fractions cannot be obtained.

It can be established that from Table 1 that 20 combustion intermediates are identified, including six radicals. Most of the identified intermediate have a much smaller molecular weight than the fuel 1,4-dioxane, and the largest intermediate is methyl vinyl ether (*m/z* 58). Aromatics including benzene are not observed in the present work, though they have been reported before.[20−22]

2. Mole Fraction Profiles of Combustion Intermediates. The mole fraction profiles of hydrocarbon intermediates are displayed in Figures 3−5. These hydrocarbon intermediates include seven stable hydrocarbons and four hydrocarbon radicals. It can be known that ethylene and acetylene have much higher concentrations than other stable hydrocarbons (allene, propyne, 1,3-butadiyne, vinylacetylene, and 1,3-butadiene) in the fuel-rich 1,4-dioxane flame. The peak mole fractions of ethylene and acetylene are 4.09×10^{-2} and 2.05×10^{-2}, respectively, whereas the peak mole fractions of other stable hydrocarbons are all lower than 2.00×10^{-3}. Meanwhile, the peak mole fractions of methyl radical and ethyl radical (including formyl radical) also have much higher concentrations than the other hydrocarbon radicals (propargyl radical and allyl radical). The peak mole fractions of methyl radical and the ethyl radical (including formyl radical) are 1.95×10^{-3} and 8.00×10^{-4}, respectively, whereas those of propargyl radical and allyl radical are 3.64×10^{-4} and 1.55×10^{-4}, respectively.

It can be seen from Figure 5 that the peak positions of 1,3-butadiene (C_4H_6), vinylacetylene (C_4H_4), and 1,3-butadiyne (C_4H_2) are 6.0, 7.5, and 9.0 mm, respectively. This shows that they form and reach the peak mole fraction in different positions in the fuel-rich 1,4-dioxane flame though have the same number of carbon atoms. For these three identified C_4-hydrocarbon

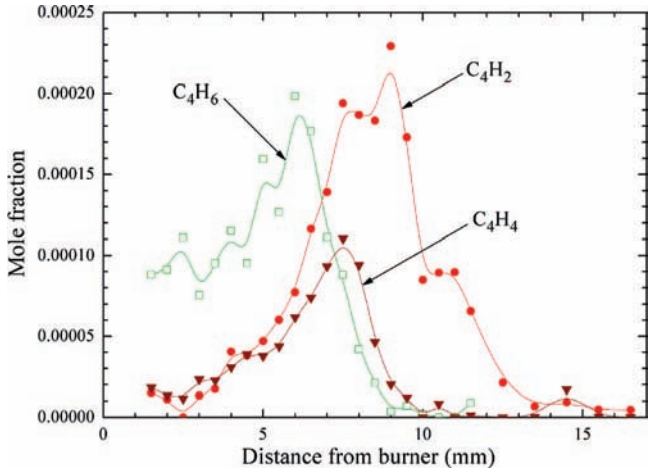

Figure 5. Mole fraction profiles of C_4-hydrocarbon intermediates in fuel-rich 1,4-dioxane flame.

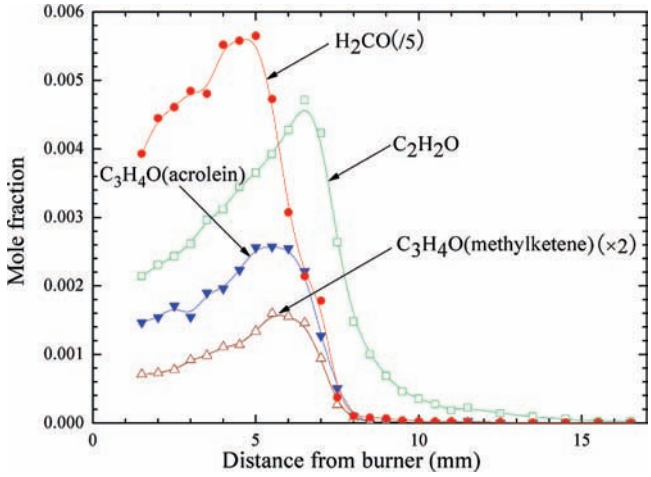

Figure 6. Mole fraction profiles of oxygenated hydrocarbon intermediates in fuel-rich 1,4-dioxane flame.

intermediates, 1,3-butadiyne has the highest degree of unsaturation and its peak position has the longest distance from the burning surface, whereas 1,3-butadiene has the lowest degree of unsaturation and its peak position occurs at the shortest distance from the burning surface. This trend can also be obtained by comparing the mole fraction profiles of ethylene (C_2H_4) and acetylene (C_2H_2), whose peak positions are 5.0 and 6.5 mm, respectively.

The above observations show that the H abstraction of hydrocarbon intermediates occurs widely in the fuel-rich 1,4-dioxane flame. The primary hydrocarbon intermediates (always with low degree of unsaturation) are not oxidized to the combustion product (CO and CO_2) immediately; on the contrary, they undergo a comparatively long and complex process. For example, C_4H_6 is deprived two hydrogen atoms to form C_4H_4 at first; C_4H_4 is again deprived two hydrogen atoms to form C_4H_2 in the second step; and C_4H_2 finally oxidized and decompose to the combustion products. These processes occur at different spatial positions in the flame, corresponding to different periods in the combustion process. This result provides valuable information about the formation routes of some hydrocarbon intermediates, which will be discussed later.

The mole fraction profiles of oxygenated hydrocarbon intermediates are displayed in Figure 6. A total of nine oxygenated hydrocarbon intermediates, including seven stable intermediates and two radicals, are identified in the fuel-rich 1,4-dioxane flame. Unfortunately, some mole fraction profiles of the identified oxygenated hydrocarbon intermediates (ethenol, acetaldehyde, ethoxy radical, and methoxyethylene) cannot be obtained as their IEs are too near to the APs of the fragment ion (with the same value of m/z) from 1,4-dioxane. The IEs of formyl radical and ethyl radical are so near that it is impossible to obtain a separate mole fraction profile for each of them under the current setup and experimental condition. Therefore, the mole fraction of formyl radical is displayed together with ethyl radical as shown in Figure 3.

Formaldehyde (H_2CO) is the smallest identified stable oxygenated hydrocarbon intermediate, which reaches the peak mole fraction of 2.82×10^{-2} at 5.0 mm. Ketene (C_2H_2O) reaches the peak mole fraction of 4.72×10^{-3} at 6.5 mm. Acrolein and methylketene have rather low concentrations, in comparison with formaldehyde and ketene. Their peak mole fractions are 2.57×10^{-3} (at 5.0 mm) and 7.99×10^{-4} (at 5.0 mm), respectively. The peak positions of oxygenated hydrocarbon intermediates distribute from 5.0 to 6.5 mm, which means that oxygenated hydrocarbon intermediates form and reach their peak mole fractions in a much earlier period than the hydrocarbon intermediates.

3. Formation Routes of Combustion Intermediates. As flames of cyclic oxygenated hydrocarbon have seldom been studied, it is significant to discuss the formation routes of combustion intermediates in fuel-rich 1,4-dioxane flame. 1,4-Dioxane has a cyclic structure, and this should result in prominent difference between 1,4-dioxane and the reported noncyclic oxygenated hydrocarbons. On the basis of the experimental results in this work, the formation routes of the observed intermediates in fuel-rich 1,4-dioxane flame are proposed in Figure 7. To put these formation routes in order, most of these intermediates are placed corresponding to their peak positions measured in the flame. For the intermediates whose peak positions are not obtained in the present work, they will be given estimated peak positions according to their formation routes. The formation of methyl radical, unlike many other intermediates, begins around 5.5 mm where the decomposition of 1,4-dioxane takes place; however, its formation has other dominant components so that its peak occurs around 7.0 mm. To make the discussions of formation routes of intermediates in an organized way, the whole flame area is divided to four zones (A−D) as shown in Figure 7.

Zone A (from 0 to 5.0 mm) is considered to be the area where the fuel 1,4-dioxane decomposes and the primary intermediates are produced. Saturated oxygenated hydrocarbon is assumed to be destroyed only by H abstraction, which is also the dominating initial step of the decomposition process.[19,21] 1,4-Dioxane is also a saturated oxygenated hydrocarbon; hence, the decomposition process should be started by H abstraction as shown in Figure 7. "X" in Figure 7 is a H acceptor, like H, O, OH, or another radical. It can be known that the intermediates from 1,4-dioxane decomposition, like ethylene, formaldehyde, and ethoxy radical, always have small molecular weight. This shows that the cyclic structure of the 1,4-dioxane molecule possibly leads to a fast and thorough decomposition process, and large intermediates (with more than two carbon atoms) rarely form in this zone. The formation of other observed intermediates can be well described through various reaction routes initiated by these three primary intermediates. The oxidizer O_2 is considered to be consumed to produce O and OH in this zone.

In zone B (from 5.0 to 5.5 mm), the primary intermediates ethylene, formaldehyde, and ethoxy radical produce new intermediates only through H abstraction or H addition. Only

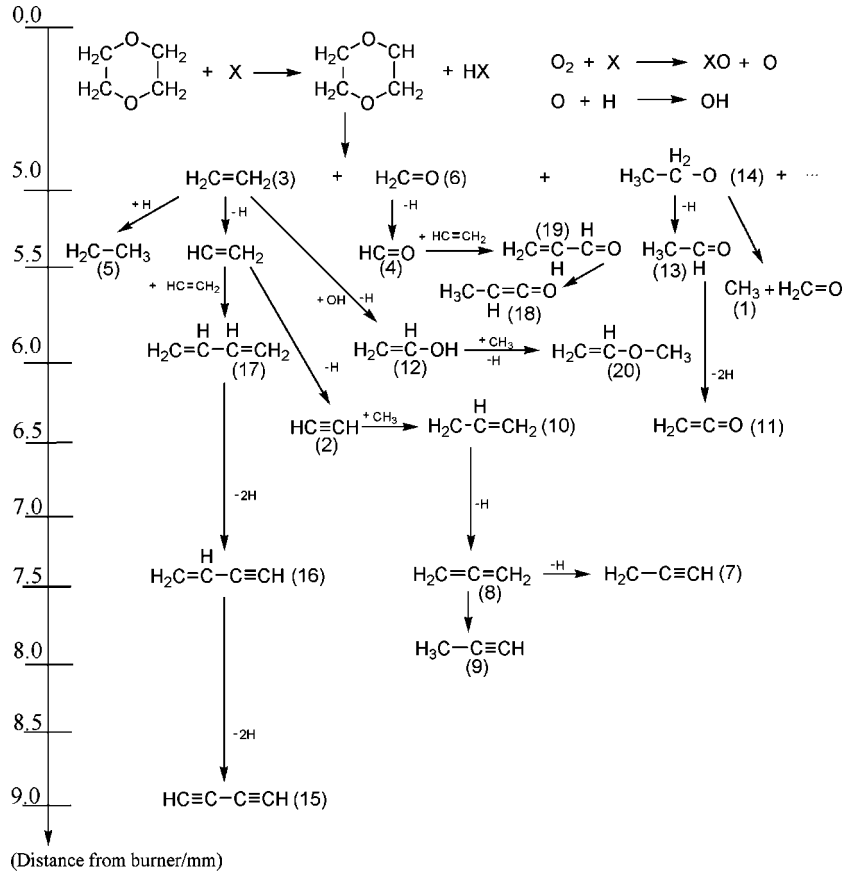

Figure 7. Formation routes of intermediates in fuel-rich 1,4-dioxane flame.

H abstraction and H addition are proved to occur in this zone, and this is the main characteristic that is different from zone C. Other kinds of reactions like recombination do not occur in this zone. Note that a complete reaction of H abstraction should be RH + X → R + XH, but it is written in brief as RH − H → R in Figure 7. In comparison with H abstraction, H additions are much more difficult to occur in this zone. All of these three primary intermediates are involved in reactions of H addition, whereas only one of them (ethylene) is involved in H abstraction, and produces ethyl radical. Several important radicals like vinyl radical, ethyl radical, and formyl radical are produced in this zone, which will play key roles in the combustion process.

Zone C (from 5.5 to 6.5 mm) should be the most complex zone among all the four zones, and about half of the intermediates form in this zone. Formation routes of intermediates in zone C contain reactions of decomposition, recombination, H abstraction, H substitution, and H migration. Methyl radical is considered to be formed in this zone from decomposition of ethoxy radical, and this should be a continued process of 1,4-dioxane decomposition. Reactions of recombination and H substitution occur in this zone so that large intermediates (with more than two carbon atoms) can form in fuel-rich 1,4-dioxane flame. For example, allyl radical forms from recombination reaction of methyl radical and acetylene, whereas methoxyethylene forms from H substitution reaction of methyl radical and ethenol. Intramolecular H migration leads to the presence of isomers, like methylketene and acrolein. Ethenol whose formation route is quite different from other oxygenated intermediates, forms through H substitution reaction of ethylene and OH as shown in Figure 7.

Zone D (from 6.5 to 9.0 mm) is much wider than zone C; however, the formation routes of the intermediates in zone D are seen to be much simpler than those in zone C. All the intermediates formed in this zone are large hydrocarbon intermediates, including four stable hydrocarbon intermediates and one hydrocarbon radical. Only H abstraction and H migration are proved to occur in this zone, and H abstraction is the dominating one. It is obvious that the process of H abstraction lasts a long period in fuel-rich 1,4-dioxane flame. For example, H abstraction of 1,3-butadiene (6.0 mm) produces vinylacetylene (7.5 mm), and H abstraction of vinylacetylene produces vinylacetylene (9.0 mm). In addition, allene converses to propyne in this zone as shown in Figure 7, and it is considered to be achieved through intramolecular H migration, as well as H-atom assisted isomerization.[31]

4. Characteristics of Combustion Intermediates. The intermediates in the fuel-rich 1,4-dioxane flame display clear characteristics by comparing with these in reported noncyclic oxygenated hydrocarbons.[20−22] First, the number of intermediate species in fuel-rich 1,4-dioxane flame is rather small. Only 20 intermediates in the 1,4-dioxane flame are identified in the present work, whereas more than 50 intermediates are identified in each flame of butanol isomers (ϕ = 1.71, C/O ratio = 0.50) using the same instrument,[20] which have the equal number of carbon atoms to 1,4-dioxane. Second, intermediates in fuel-rich 1,4-dioxane flame have rather small molecular weight. For example, the largest hydrocarbon intermediate identified in fuel-rich 1,4-dioxane flame is 1,3-butadiene (m/z 54), whereas the largest hydrocarbon intermediates in fuel-rich flames of ethyl formate (ϕ = 1.82, C/O ratio = 0.51), isopropyl alcohol (ϕ = 1.80, C/O ratio = 0.50), and butanol are benzene (m/z 78),[22] toluene (m/z 92),[21] and ethylbenzene (m/z 106),[20] respectively. Third, the concentrations of C_3 and C_4 intermediates (both hydrocarbon intermediates and oxygenated hydrocarbons inter-

mediates) are much lower than those of C_1 and C_2 intermediates in the fuel-rich 1,4-dioxane flame. For example, the concentration of acetylene is 2.05×10^{-2}, about 130 times higher than that of propyne (1.55×10^{-4}). Fourth, aromatic species including benzene are absent in the fuel-rich 1,4-dioxane flame. The absence of aromatics is a prominent difference between the fuel-rich 1,4-dioxane flame and previously studied fuel-rich flames of noncyclic oxygenated hydrocarbons. A series of aromatics, like benzene, toluene, styrene, ethylbenzene, and *p*-xylene were observed in the noncyclic oxygenated hydrocarbons flames.

The characteristics of intermediates in fuel-rich 1,4-dioxane flame are closely related to the molecule structure of fuel 1,4-dioxane. Recently, Westbrook et al. used detailed chemical modeling to study suppression of sooting in diesel engines by oxygenated additives.[32] This modeling showed that the soot-suppression efficiencies of the oxygenated species depended on their molecular structure. The absence of high molecular weight intermediates and aromatics in 1,4-dioxane flame can be well explained based on this modeling. 1,4-Dioxane molecule contains two oxygen atoms, and they are not connected to the same carbon atom; hence, each of them can remove one carbon from the precursor pool of high molecular weight intermediates including aromatics.[32] In addition, in comparison with an equivalent saturated noncyclic oxygenate, 1,4-dioxane has less hydrogen atoms because of the cyclic structure. Therefore, less oxygen atoms are consumed to produce H_2O, and more oxygen atoms are available to prevent carbon atoms from producing precursors of high molecular weight intermediates.

On the basis of the discussion above, the low concentrations of C_3 and C_4 intermediates in fuel-rich 1,4-dioxane flame are easy to understand, since they are important potential members of the precursor pool. As formation of some precursors is restrained and their concentrations are very low in the fuel-rich 1,4-dioxane flame, many intermediates, especially high molecular weight species including aromatics, are absent. Correspondingly, the number of the intermediate species detected in fuel-rich 1,4-dioxane flame is rather small, because of the absence of these intermediates.

5. Evaluation of Pollutant Emissions from 1,4-Dioxane Combustion. In the previous investigation, it is concluded that the combustion of oxygenated hydrocarbon can reduce particulate emissions,[2,33] but it has potential emission of toxic byproduct.[34] Unfortunately, these conclusions are mainly based on the studies of noncyclic oxygenated hydrocarbons. Therefore, evaluation of pollutant emissions from 1,4-dioxane combustion is very necessary.

Four light toxic molecules, including one hydrocarbon (1,3-butadiene) and three oxygenated hydrocarbons (formaldehyde, acetaldehyde, and acrolein), are identified in fuel-rich 1,4-dioxane flame. 1,3-Butadiene is considered to be a hazardous air pollutant by the 1990 U.S. Clean Air Act, and its cancer risk potency is over 25 times higher than that of benzene.[35] Formaldehyde and acetaldehyde are considered to be the main toxic byproducts from oxygenated hydrocarbons combustion, and they have been widely observed. Both of them are allergens and respiratory irritants, while formaldehyde is also a probable human carcinogen and acetaldehyde is also an eye irritant. Acrolein, however, has seldom been observed in the previous studies of noncyclic oxygenated hydrocarbons. Acrolein is a severe pulmonary irritant and lacrimating agent. Other toxics of oxygenated hydrocarbons, like methanol and methyl ethyl ketone, are not observed in the fuel-rich 1,4-dioxane flame.

Many aromatics are considered to be the air toxic pollutants that associated with the combustion process, and soot particles are thought to pose a particularly great risk to health. For example, benzene is a probable human carcinogen which can cause leukemia.[34] Different from the previous reports about the fuel-rich flames of noncyclic oxygenated hydrocarbons, no aromatics are observed in the fuel-rich 1,4-dioxane flame. Furthermore, the absence of aromatics may make the formation of PAHs difficult, and thus the soot emissions from 1,4-dioxane combustion are possibly avoided.

Conclusion

A fuel-rich premixed laminar 1,4-dioxane/O_2/Ar flame at low pressure (30 Torr) with an equivalence ratio of 1.80 was studied in the present work. A total of 20 combustion intermediates were identified with the tunable synchrotron VUV photoionization and MBMS technique, and the mole fraction profiles of most intermediates are obtained. Aromatics including benzene are not observed, and the concentrations of C_3 and C_4 intermediates are much lower than those of C_1 and C_2 intermediates. The characteristics of intermediates mentioned above can be well explained via the high symmetry and cyclic structure of the 1,4-dioxane molecule. Formation routes of the intermediates are proposed based on their measured peak positions. A discussion of the pollutant emissions show some light molecules are formed from the 1,4-dioxane combustion; however, toxic aromatics and soot particles emission are possibly avoided.

Acknowledgment. The authors are grateful to Professor Fei Qi for providing beam time to perform the experiments at the National Synchrotron Radiation Laboratory. This work is supported by the National Nature Science Foundation of China (No. 50476025).

References and Notes

(1) Curran, H. J.; Pitz, W. J.; Westbrook, C. K.; Dagaut, P.; Boetter, J. C.; Cathonnet, M. *Int. J. Chem. Kinet.* **1998**, *30*, 229.
(2) Beatrice, C.; Bertoli, C.; Giacomo, N. D. *Combust. Sci. Technol.* **1998**, *137*, 31.
(3) Fisher, E. M.; Pitz, W. J.; Curran, H. J.; Westbrook, C. K. *Proc. Combust. Inst.* **2000**, *28*, 1579.
(4) Kitamura, T.; Ito, T.; Senda, J.; Fujimoto, H. *JSAE Rev.* **2001**, *22*, 139.
(5) McEnally, C. S.; Pfefferle, L. D. *Int. J. Chem. Kinet.* **2004**, *36*, 345.
(6) Ergut, A.; Granata, S.; Jordan, J.; Carlson, J.; Howard, J. B.; Richter, H.; Levendis, Y. *Combust. Flame* **2006**, *144*, 757.
(7) Metcalfe, W. K.; Dooley, S.; Curran, H. J.; Simmie, J. M.; El-Nahas, A. M.; Navarro, M. V. *J. Phys. Chem. A* **2007**, *111*, 4001.
(8) Gail, S.; Thomson, M. J.; Sarathy, S. M.; Syed, S. A.; Dagaut, P.; Dievart, P.; Marchese, A. J.; Dryer, F. L. *Proc. Combust. Inst.* **2007**, *31*, 305.
(9) Sarathy, S. M.; Gail, S.; Syed, S. A.; Thomson, M. J.; Dagaut, P. *Proc. Combust. Inst.* **2007**, *31*, 1015.
(10) Dagaut, P.; Gail, S.; Sahasrabudhe, M. *Proc. Combust. Inst.* **2007**, *31*, 2955.
(11) Dooley, S.; Curran, H. J.; Simmie, J. M. *Combust. Flame* **2008**, *153*, 2.
(12) Herbinet, O.; Pitz, W. J.; Westbrook, C. K. *Combust. Flame* **2008**, *154*, 507.
(13) Cool, T. A.; Nakajima, K.; Mostefaoui, T. A.; Qi, F.; McIlroy, A.; Westmoreland, P. R.; Law, M. E.; Poisson, L.; Peterka, D. S.; Ahmed, M. *J. Chem. Phys.* **2003**, *119*, 8356.
(14) Cool, T. A.; McIlroy, A.; Qi, F.; Westmoreland, P. R.; Poisson, L.; Peterka, D. S.; Ahmed, M. *Rev. Sci. Instrum.* **2005**, *76*, 094102.
(15) Qi, F.; Yang, R.; Yang, B.; Huang, C. Q.; Wei, L. X.; Wang, J.; Sheng, L. S.; Zhang, Y. W. *Rev. Sci. Instrum.* **2006**, *77*, 084101.
(16) Taatjes, C. A.; Hansen, N.; Osborn, D. L.; Kohse-Hoinghaus, K.; Cool, T. A.; Westmoreland, P. R. *Phys. Chem. Chem. Phys.* **2008**, *10*, 20.
(17) Marr, L. C.; Kirchstetter, T. W.; Harley, R. A. *Environ. Sci. Technol.* **1999**, *33*, 3091.
(18) Al-Farayedhi, A. A. *Int. J. Energy Res.* **2002**, *26*, 279.

(19) Cool, T. A.; Wang, J.; Hansen, N.; Westmoreland, P. R.; Dryer, F. L.; Zhao, Z.; Kazakov, A.; Kasper, T.; Kohse-Hoinghaus, K. *Proc. Combust. Inst.* **2007**, *31*, 285.

(20) Yang, B.; Osswald, P.; Li, Y. Y.; Wang, J.; Wei, L. X.; Tian, Z. Y.; Qi, F.; Kohse-Hoinghaus, K. *Combust. Flame* **2007**, *148*, 198.

(21) Li, Y. Y.; Wei, L. X.; Tian, Z. Y.; Wang, J.; Zhang, T. C.; Qi, F. *Combust. Flame* **2008**, *152*, 336.

(22) Osswald, P.; Struckmeier, U.; Kasper, T.; Kohse-Hoinghaus, K.; Wang, J.; Cool, T. A.; Hansen, N.; Westmoreland, P. R. *J. Phys. Chem. A* **2007**, *111*, 4093.

(23) Battin, F.; Scacchi, G.; Baronnet, F. *Int. J. Chem. Kinet.* **1991**, *23*, 861.

(24) Yang, B.; Li, Y. Y.; Wei, L. X.; Huang, C. Q.; Wang, J.; Tian, Z. Y.; Yang, R.; Sheng, L. S.; Zhang, Y. W.; Qi, F. *Proc. Combust. Inst.* **2007**, *31*, 555.

(25) Cool, T. A.; Nakajima, K.; Taatjes, C. A.; McIlroy, A.; Westmoreland, P. R.; Law, M. E.; Morel, A. *Proc. Combust. Inst.* **2005**, *30*, 1681.

(26) Cool, T. A.; Wang, J.; Nakajima, K.; Taatjes, C. A.; McIlroy, A. *Int. J. Mass Spectrom.* **2005**, *247*, 18.

(27) Robinson, J. C.; Sveum, N. E.; Neumark, D. M. *J. Chem. Phys.* **2003**, *119*, 5311.

(28) Robinson, J. C.; Sveum, N. E.; Neumark, D. M. *Chem. Phys. Lett.* **2004**, *383*, 601.

(29) Koizumi, H. *J. Chem. Phys.* **1991**, *95*, 5846.

(30) Linstrom, P. J.; Mallard, W. G. *NIST Chemistry Webbook*; National Institute of Standards and Technology: Gaithersburg, MD, 2005 (http://webbook.nist.gov).

(31) Miller, J. A.; Senosiain, J. P.; Klippenstein, S. J.; Georgievskii, Y. *J. Phys. Chem. A* **2008**, *112*, 9429.

(32) Westbrook, C. K.; Pitz, W. J.; Curran, H. J. *J. Phys. Chem. A* **2007**, *110*, 6912.

(33) Song, K. H.; Nag, P.; Litzinger, T. A.; Haworth, D. C. *Combust. Flame* **2003**, *135*, 341.

(34) Koshland, C. P. *Proc. Combust. Inst.* **1996**, *26*, 2049.

(35) Riservato, M.; Rolla, A.; Davoli, E. *Rapid Commun. Mass Spectrom.* **2004**, *18*, 399.

JP8098895